Bioactive effects of natural and novel unnatural tropolone sesquiterpenoids in a murine cell model of renal interstitial fibroblasts

*Timna C. Bergmann[1], Max Menssen[2], Carsten Schotte[3], Russell J. Cox[3], Cornelia Lee-Thedieck[1]**

T.C. Bergmann, Prof. Dr. C. Lee-Thedieck

[1] Institute of Cell Biology and Biophysics, Department of Cell Biology, Leibniz University Hannover, 30419 Hannover, Germany

Dr. M. Menssen

[2] Institute of Cell Biology and Biophysics, Department of Biostatistics, Leibniz University Hannover, 30419 Hannover, Germany

Dr. C. Schotte, Prof. Dr. R.J.Cox

[3] Institute of Organic Chemistry and BMWZ, Leibniz University Hannover, 30167 Hannover, Germany

* Prof. Dr. Cornelia Lee-Thedieck, Leibniz University Hannover, Institute of Cell Biology and Biophysics, Herrenhäuserstr 2, 30419 Hannover. Phone: +49 511 762 14 972; Fax: +49 511 762 2606; Email: lee-thedieck@cell.uni-hannover.de

ABSTRACT

Fungal specialized metabolites are known for their potent biological activities, and among them, tropolone sesquiterpenoids (TS) stand out for their diverse bioactive properties. Here, we explored the bioactivity of the novel TS compounds 4-hydroxyxenovulene B and 4-dehydroxy norpycnidione, along with the structurally related compounds 4-hydroxy norxenovulene B and xenovulene B, and compared them to the well-established TS compounds eupenifeldin and pycnidione. Exposure to TS compounds induced notable changes in cell shape and branching patterns. These changes correlated upon treatment with structurally similar compounds and were associated with the presence of tropolone moieties in the molecules. The survival of the renal interstitial fibroblast-derived FAIK3-5 cell line was significantly impacted by the number of tropolone moieties, with dual-substituted compounds showing higher cytotoxicity compared to those with a single tropolone substitution. Treatment with eupenifeldin, 4-hydroxyxenovulene B and 4-dehydroxy norpycnidione had diverse effects on cellular behavior and reduced erythropoietin content in hypomethylated FAIK3-5 cells. Moreover, 4-dehydroxy norpycnidione elicited reduced proliferation with minimal cytotoxicity and holds promise as a potential candidate for further (pre-)clinical testing in cancer treatment. Our findings represent a step forward in understanding how the molecular structures of bioactive TS compounds are connected to their biological effects, potentially enhancing their clinical applicability.

INTRODUCTION

Natural products and their structural analogues have long been valuable sources of medical products due to their diverse chemical architectures and structural complexity. These active ingredients are categorized into primary and secondary (or specialized) metabolites [1,2]. Specialized metabolites are structurally diverse and are often optimized for specific biological functions. Advances in screening, isolation, and characterization methods for these metabolites have led to the discovery and development of novel drugs against various diseases [3–6] including cancer [7,8], as well as treatments for drug-resistant infections [9,10]. However, the number of unexplored compounds, especially in fungi, remains high [11], despite recent progress in screening and characterization strategies. The potential of specialized metabolites to target persistent medical care challenges remains significant [12].

One promising family of bioactive fungal specialized metabolites are tropolone sesquiterpenoids (TS). In 1993 the bistropolone pycnidione **1** [13] and its diastereomer eupenifeldin **2** [14] were the first reported TS compounds. They display a wide variety of diverse biological activities. For example, eupenifeldin (**2)** was isolated from *Eupenicillium brefeldianum* as an antitumor agent against human HTC colon carcinoma cell lines [14], and further cytotoxic effects were recorded vs several human cell lines [15,16]. Eupenifeldin (**2**) also displays antifungal properties (vs *Candida albicans*) and antimalarial activity (vs *Plasmodium falciparum* K1) [15]. Similarly, reported activities of the structurally related TS compound pycnidione (**1**), first isolated from an unidentified *Phoma* sp. [13], include anticancer activities [17–19], as well as weak antibacterial [20] and antimalarial properties [17,20,21]. Pycnidione (**1**) is part of the "epolone family" of TS, known for the induction of erythropoietin (EPO) gene expression in HRCHO5, HepG2 and Hep3B reporter cell lines [22,23]. Over the last decades a variety of bioactivities of other TS compounds,

most of which belong to the eupenifeldin series, has been discovered [24–28], however, no such activities have been reported yet for the monotropolones xenovulene B **3,** first reported in 1997 [29] and fully characterized by Schor et al. [30], and 4-hydroxyxenovulene B **4** [31].

TS compounds are a unique class of fungal meroterpenoids with a conserved core structure consisting of a humulene-derived macrocycle and pendent tropolones connected via one or two dihydropyran rings (Fig. 5). Chemical diversity in TS metabolizing fungi is due to variances in fungal biosynthetic gene clusters (BGCs), which encode metabolite synthesis. The exact determination of the stereochemistry of TS has been difficult and has only recently been accurately reassigned [32,33]. Redesigning and refactoring known BGCs and effective heterologous expression in engineered hosts like *A. oryzae* NSAR1 can accelerate the synthesis process of TS compounds and create platforms for new compound discovery. Combining genes of known BGCs can create new specialized metabolites with specific characteristics and bioactivities [34]. Previously, Schotte et al. described the successful isolation and identification of several TS compounds, including xenovulene B (**3**), 4-hydroxyxenovulene B (**4**) as well as the two hitherto unknown compounds 4-dehydroxy norpycnidione **5** and 4-hydroxy norxenovulene B **6** by recombining genes of three key TS BGC in *A. oryzae* NSAR1 [30,31]. To date, no biological activity of these compounds has been reported in the literature but given the high potency of structurally related TS compounds such as pycnidione (**1**) and eupenifeldin (**2**), similar effects on cellular mechanisms can be expected.

The known physiological effects of TS compounds include hypoxia-independent activation of EPO gene expression in reporter cell lines Hep3B [22], HepG2, and HRCHO5 [23] after treatment with pycnidione (**1**). However, early drug discovery studies often used genetically engineered cell lines that cannot reflect physiological conditions, or rely on indirect measurements, putatively

leading to false-positive results due to assay interferences [35]. To improve the quality of early *in vitro* drug testing studies, protein expression analysis in a system more similar to natural conditions would be beneficial and lead to more reliable results. EPO is mainly produced by fibroblastoid renal erythropoietin-producing (REP) cells and is highly regulated at the transcriptional level [36]. Therefore, a sustainable and simplified model for EPO *in vitro* studies is desirable. Recently, Imeri et al. introduced an immortalized clonal cell line derived from mouse REP cells called FAIK3-5 that can produce erythropoietin for at least 30 passages [37]. By using this cell line to test the bioactivity of the newly discovered TS and related compounds [31] (Fig. 5), we are closer to a physiological model than when using cell lines derived from liver tissue, and also meet the necessary requirements for toxicological and cell proliferation studies.

Morphological profiling is crucial in lead identification to assess, if compounds cause morphological changes related to cell adhesion, proliferation, or viability [38–40]. Cellular morphology is influenced by dynamic interactions between cytoskeleton, membrane, and adhesion complexes. Regulatory signal transduction systems convert external cues into biochemical signals for cell adaptation [41]. Cell phenotypes therefore combine observable characteristics with biochemical properties and gene and protein expression. However, standardized morphometric descriptors and analysis tools are needed to mitigate subjective evaluation and reveal information not readily apparent from visual inspection [42].

In this study we aim to use standardized morphometric and two-dimensional branching descriptors to identify differences in cell shapes and ramification patterns [42,43] in FAIK3-5 cells treated with the novel TS compounds **4** and **5**, as well as with the structurally related **compounds 3** and **6**, for which no bioactive effects have been reported. By comparison with the well characterized bioactive compounds **1** and **2**, we aim to find a link between the molecular structures

of related TS compounds and their biological effects. This could help to decipher the biological functions of TS moieties and support synthetic biology approaches for redesigning TS compounds, ultimately improving drug efficacy and potential clinical applications.

RESULTS

Structurally related tropolone sesquiterpenoids promote similar morphological alterations in FAIK3-5 cells

Substantial alterations in cell morphologies are frequently observed during screening studies of natural or synthetic compounds [38,44]. Correspondingly, we found significant changes in cell morphologies of TS compound treated samples compared to untreated control samples, correlating in samples treated with compounds with structural similarity.

Compound treatment showed either no effect on cell growth and morphology (compound **6**), or a prominent modification of cellular shapes in a dose-independent manner after treatment with tropolone-bearing compounds (compounds **1**-**5**) (Supplementary Fig. S1). Samples treated with 4-hydroxyxenovulene B (**4**) additionally revealed lower cell confluency at a concentration of 12 µM compared to samples treated with lower concentrations.

Treatment with the two bistropolones (**1**, **2**) caused a neuron-like morphology in FAIK3-5 cells, while monotropolones (**3**, **4** and **5**) resulted in epithelial-like cell morphology. The cells treated with compound **6** that lacks a tropolone moiety displayed a more elongated, fibroblast-like morphology that resembles the natural morphology of untreated FAIK3-5 cells. Furthermore, we observed the emergence of flat and enlarged cells, which were highly granulated, in all treatment conditions with tropolone-containing compounds **1-5** (Fig. 1 **a**). Notably, the tropolone-lacking compound 4-hydroxy norxenovulene B (**6**) exhibited no alteration in cell morphology or growth

inhibition, suggesting that tropolone moieties are responsible for changes of cell phenotype and proliferation (Supplementary Fig. S1).

Based on this observation we hypothesized that treatment with structurally related TS compounds might trigger similar biochemical responses in FAIK3-5 cells, resulting in comparable phenotypes. Multiple comparison tests on shape descriptors and morphometric parameters (cell area, aspect ratio (AR), perimeter, relative protrusion area (= *solidity*), length of protrusions (= *circularity*) as well as number of protrusions and branches) were performed to detect putative morphological similarities between the TS-treated cells (Fig. 1 **b**). As all applied statistical analysis models depend on variables that were measured on the same cell, multiple contrast tests were carried out with respect to the correlations between dependent variables using multiple marginal models [45,46] (Supplementary Information S9 and S10). For the sake of better visualization of the morphological appearance of cells, differently treated and untreated FAIK3-5 samples were illustrated with the Matlab (Version R2021b) toolbox PhenoPlot [47]. Visualized plots concur with the conducted multiple comparison analysis (Fig. 1 **c**), which reveal no significant differences ($p > 0.05$) between tested shape descriptors and morphometric parameters in samples treated either with bistropolones (**1**, **2**) or monotropolones (**3**, **4**). Contrarily, the treatment with unrelated compounds led to significant morphological differences between analysed cell samples. Cells treated with the compound 4-dehydroxy norpycnidione (**5**), which belongs to the xenovulene-/ pycnidione-type TS, characterized by the trans-fusion at C-8/C-9 position of the central α-humulene derived macrocycle, show a higher morphological equivalence to cells treated with the structurally distinct TS compounds xenovulene B (**3**) and 4-hydroxyxenovulene B (**4**) than to any of the other investigated compounds. Cells treated with 4-dehydroxy norpycnidione (**5**) are significantly morphologically altered only in regard of their measured AR ($p \leq 0.001$), whereas 4-

hydroxyxenovulene B (**4**) treatment additionally induces significant changes in cell area ($p \leq 0.001$) and length of protrusions ($p \leq 0.05$).

With this we can show that observed alterations in cell growth and morphology strongly relate to the tropolone moieties present on the molecules, which seem to be responsible for their bioactivity. This is additionally validated by the lack of biological responses after 4-hydroxy norxenovulene B (**6**) treatment and the high morphological similarity of mono- and bistropolone treated cells.

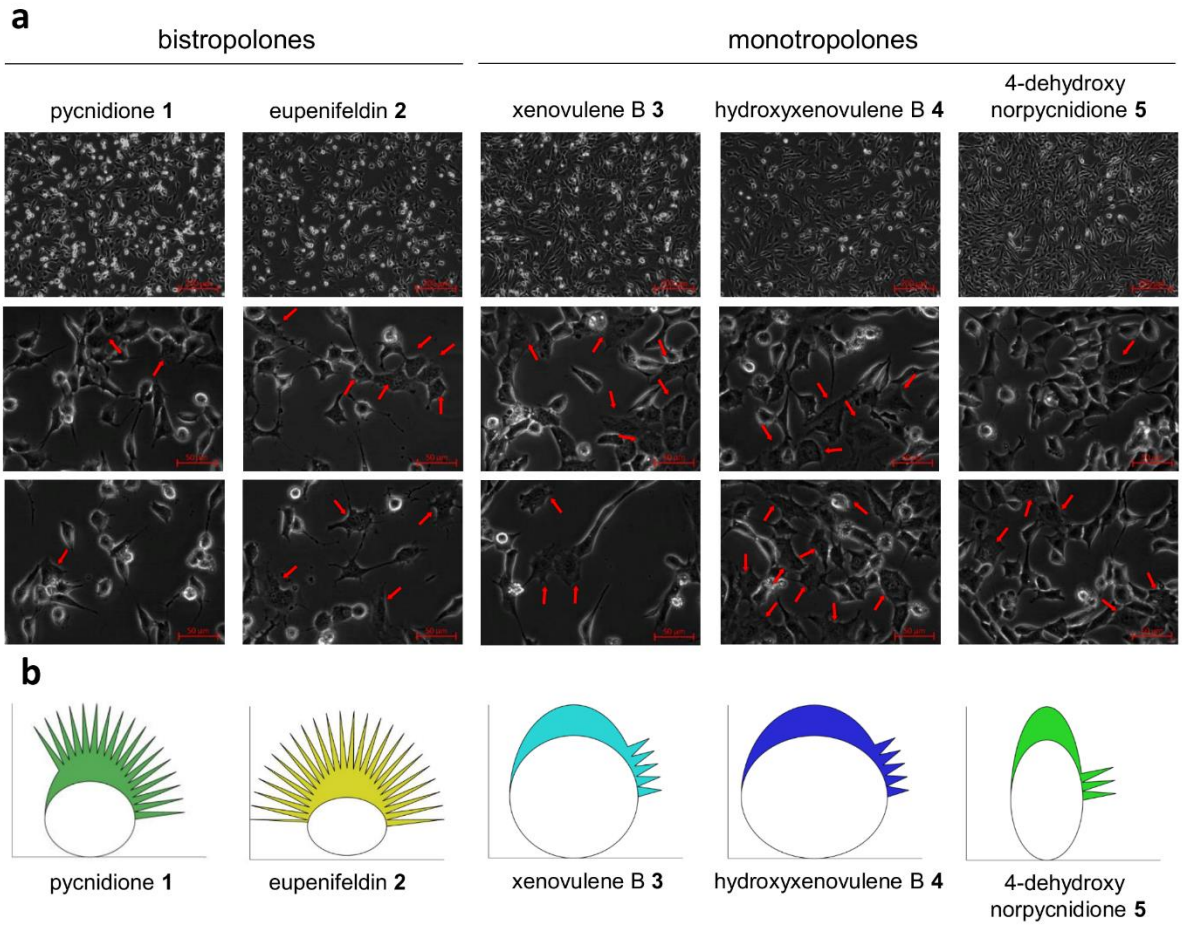

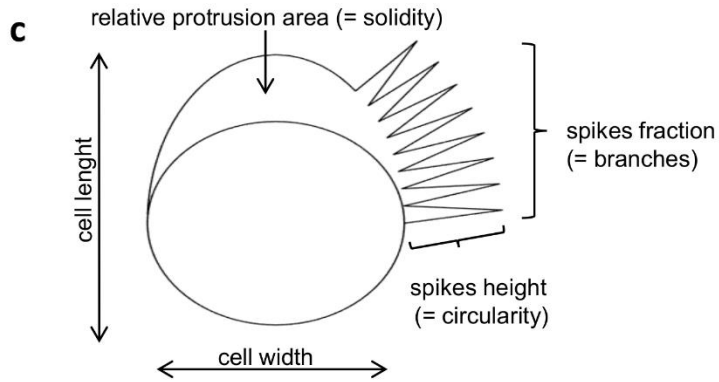

	cell area†	aspect ratio	perimeter†	solidity	circularity = length of protrusions	branches = number of protrusions	junctions†
xenovulene B **3** vs. eupenifeldin **2**	NS	NS	***	***	***	***	***
xenovulene B **3** vs. 4-dehydroxy norpycnidione **5**	NS	***	NS	NS	NS	NS	NS
xenovulene B **3** vs. hydroxyxenovulene B **4**	**NS**	**NS**	**NS**	**NS**	**NS**	**NS**	**NS**
xenovulene B **3** vs. pycnidione **1**	NS	NS	***	***	***	***	***
eupenifeldin **2** vs. 4-dehydroxy norpycnidione **5**	*	***	***	***	**	***	***
eupenifeldin **2** vs. hydroxyxenovulene B **4**	NS	NS	***	***	***	***	***
eupenifeldin **2** vs. pycnidione **1**	**NS**	**NS**	**NS**	**NS**	**NS**	**NS**	**NS**
4-dehydroxy norpycnidione **5** vs. hydroxyxenovulene B **4**	***	***	NS	NS	*	NS	NS
4-dehydroxy norpycnidione **5** vs. pycnidione **1**	NS	***	***	***	*	***	***
hydroxyxenovulene B **4** vs. pycnidione **1**	***	NS	***	***	***	***	***

Figure 1: Alterations of cell morphology of FAIK3-5 cells after 24 h of treatment with the TS compounds pycnidione (**1**), eupenifeldin (**2**)**,** xenovulene B (**3**), 4-hydroxyxenovulene B (**4**) and 4-dehydroxy norpycnidione (**5**). **(a)** Brightfield images (1 x 10x and 2 x 20x resolution from top to bottom) of samples treated for 24h with compound **1**-**5**. Red arrows indicate enlarged, flat and highly granulated cells that were visible to varying degrees in each treated sample. **(b)** Visualization of TS-treated cells in PhenoPlot, in which quantifiable cell features such as cell width and length, relative area of protrusions as well as their proportion and size (spike fraction and spike height) are displayed for each sample condition. In order to emphasize main differences between different treatments relative protrusion areas, spike fractions and spike height are coloured in dark green (pycnidione (**1**)), yellow (eupenifeldin (**2**)), light blue (xenovulene B (**3**)), dark blue (4-hydroxyxenovulene B (**4**)) and light green (4-dehydroxy norpycnidione (**5**)). **(c)** Multiple comparison analysis for analysed shape descriptors and morphometric parameters (cell area, aspect ratio, perimeter, relative protrusion area as well as length and number of protrusions/branches and branch junctions) were measured on at least 20 cells of pictures from three independent experiments in Fiji (version 1.53c). Statistical analysis of data was conducted with R (version 4.2.1). All parameters marked with (†) are not depicted in PhenoPlot graphs. Significances range from $p > 0.05$ (NS), 0.05 - 0.01 (*), < 0.01 - 0.001 (**) to < 0.001 (***). The estimated contrasts and corresponding confidence intervals are given in Supplementary Information S9 and S10.

Tropolone moieties induce a downshift of cell proliferation and increased cytotoxicity upon dual-substitution

Cytoskeletal alterations, such as irregular cell shapes and micronuclei formation, can indicate cytotoxic responses or cytostatic effects [44,48,49]. We analyzed the effects of TS compounds on proliferation and cytotoxicity in CTV stained FAIK3-5 cells, aiming to determine if the observed changes in cell morphology are accompanied by proliferative inhibition, as previously described for lung cancer cells treated with pycnidione (**1**) [19].

The concentration dependency of the proliferative inhibition of selected compounds was evaluated by treatment of the CTV stained cells with 4 µM, 6 µM, 8 µM and 12 µM for 24 h and subsequent analysis of mean fluorescence intensity (MFI) decrease resulting from cell proliferation, with decreased MFI signals corresponding to increased proliferation. (Supplementary Fig. S2 and Supplementary Table S3).

We observed increased MFI values compared to untreated samples (2.26 ± 0.4-fold higher) indicating a concentration independent proliferative deceleration of FAIK3-5 cells after treatment with compounds **1-3** and **5**. For 4-hydroxyxenovulene B (**4**), a dose-dependent decrease in proliferation was observed, with the highest decline at a compound concentration of 12 µM (2.62-fold higher than untreated samples, Supplementary Table S3). 4-dehydroxy norxenovulene B (**6**) showed no bioactivity in terms of proliferation inhibition, only a slight decrease in cell growth was observed. (Supplementary Fig. S4, Supplementary Table S3 and Supplementary Information S11). To exclude potential solvent effects, we analyzed the effects of DMSO vehicle controls (0.4 % (*v/v)*, 0.6 % (*v/v*), 0.8 % (*v/v*) and 1.2 % (*v/v*)), and 4-hydroxy norxenovulene B (**6**) in the concentrations also used for compound treatment (4 µM, 6 µM, 8 µM and 12 µM) on FAIK3-5 cells. No significant changes in morphological alteration or growth inhibition in the DMSO treated cells compared to 4-hydroxy norxenovulene B (**6**) could be detected (Supplementary Fig. S1 and Fig. S4). However, effects on cell growth were observed in samples treated with 1.2 % (*v/v*) DMSO or 8 - 12 µM 4-hydroxy norxenovulene B (**6**) in comparison to the untreated samples. Nevertheless, the percentage of proliferation deceleration was rather small in both the vehicle control (8.64 ± 3.72 % after 1.2 % (*v/v*) treatment), and tropolone-lacking compound treated samples (4.91 ± 4.43 % after 8 µM treatment and 7.64 ± 3.66 % after 12 µM treatment) when compared to samples

treated with TS compounds (129.95 ± 37.88 % and 143.52 ± 41.78 %) in the respective concentrations (Supplementary Table S3).

Following comparative experiments focused on differences in proliferative behaviour of FAIK3-5 cells after treatment with 6 µM of the bistropolones (**1**, **2**) or compound **3**, 12 µM of the monotropolones (**4**, **5**), and their respective DMSO vehicle controls. The selected concentrations emanate from previous studies [22,23] and the effects observed in the preceding experiments (Supplementary Fig. S1 and S2, Supplementary Table S3 and Supplementary Information S12). Treatment with all utilized TS compounds led to a significantly decreased proliferation rate in treated cells compared to the untreated control ($p < 0.001$), as shown by their low MFI values and shifts to lower fluorescence intensities (Fig. 2 **a**, **b**). The tropolone moiety lacking compound 4-hydroxy norxenovulene B (**6**) had no measurable effect on FAIK3-5 growth ($p = 0.951$) and showed a significant difference in MFI values compared to all samples treated with TS compounds ($p > 0.001$, Fig. 2 **a**, **c**). Moreover, as there were no detectable differences between the different tropolone-bearing compounds (Fig. 2 **b**), these results strongly indicate a key role of the tropolone-moiety in proliferation inhibition, independent of its single or dual substitution to the central 11-membered α-humulene-derived core structure of the compounds.

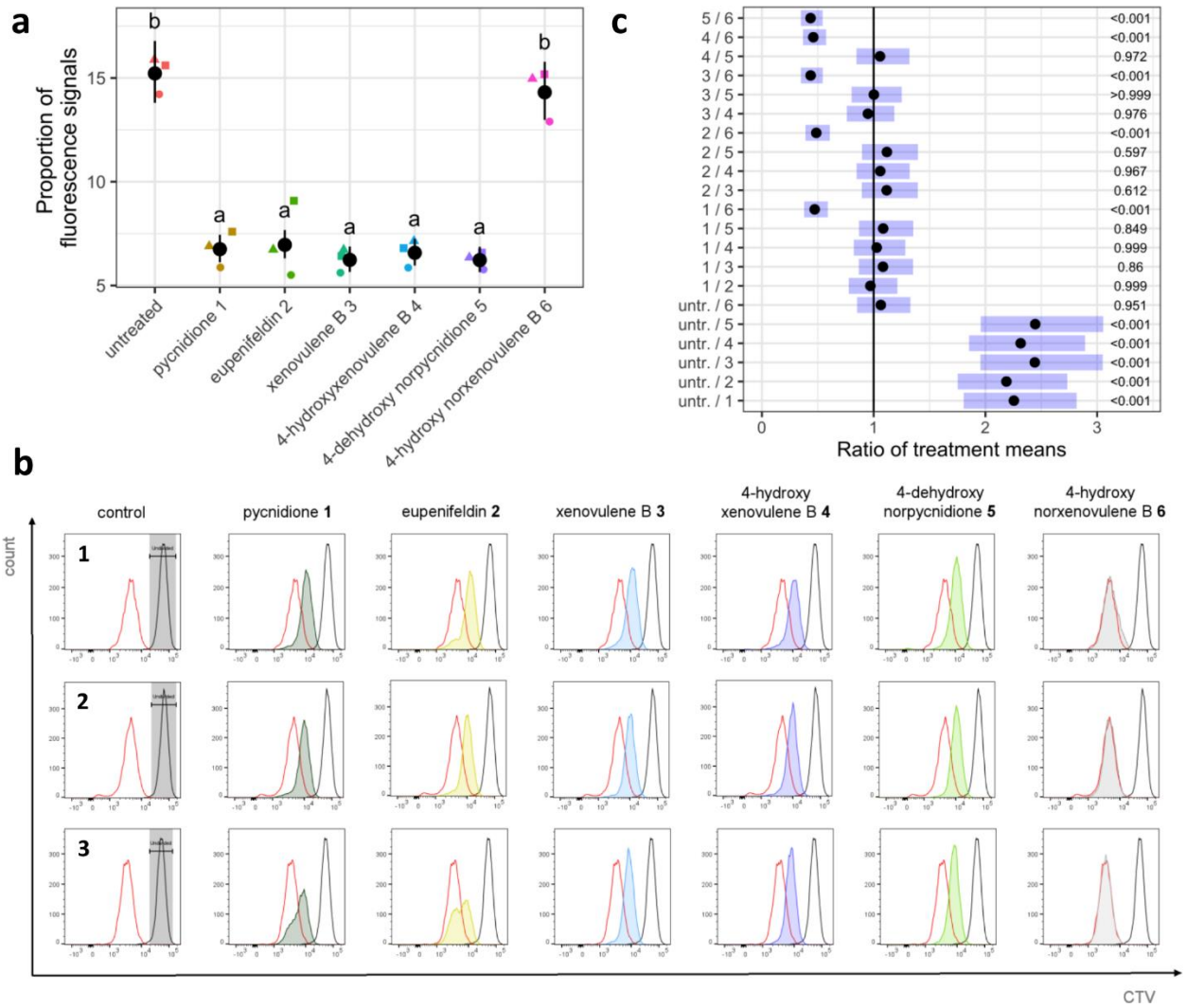

Figure 2: Proliferation deceleration of FAIK3-5 cells after treatment with pycnidione (**1**), eupenifeldin (**2**), xenovulene B (**3**), 4-hydroxyxenovulene B (**4**) and 4-dehydroxy norpycnidione (**5**) compared to untreated controls and tropolone moiety lacking compound 4-hydroxy norxenovulene B (**6**). Statistics were calculated based on normalized values of obtained ln-transformed mean fluorescence intensities (MFIs) directly after cell trace violet (CTV) staining of the undivided population and 24h post compound treatment. **(a)** Graphical overview show normalized MFI values of three biological replicates (● = 1, ▲ = 2, ■ = 3) after treatment with compounds **1** - **6** and the untreated control sample, as well as their modelled means (black dots) and pointwise 95% confidence intervals. Treatments marked with the same letter do not differ significantly from each other ($\alpha = 0.05$). **(b)** Histograms and obtained fluorescence intensities of CTV stained FAIK3-5 cells show MFI peaks and values of starting intensities of undivided cell

populations at d1 (grey background), control peaks of untreated samples at d3 (red) and MFI peaks of the respective compounds used for treatment (dark green = pycnidione (**1**), yellow = eupenifeldin (**2**), light blue = xenovulene B (**3**), dark blue = 4-hydroxyxenovulene B (**4**), light green = 4-dehydroxy norpycnidione (**5**), 4 grey = 4-hydroxy norxenovulene B (**6**)). **(C)** Pairwise mean comparisons showed significant differences in normalized MFI values between all TS compounds treated cells compared to untreated controls and compound 4-hydroxy norxenovulene B (**6**). Black dots indicate back transformed means of calculated ratios and their 95% confidence intervals (blue bars). Respective p-values for each calculation are displayed on the right side. The estimated contrasts and corresponding confidence intervals are given in Supplementary Information S11 and S12.

To investigate the potential cytotoxicity of compounds **1 - 6** and vehicle controls, their effects on FAIK3-5 cell survival was analysed via SYTOX™ AADvanced™ staining. Significances were calculated via pairwise mean comparison analysis on logit scale based on odds ratios calculated from the number of living and dead cells per analysed sample (sample size = 10.000 cells) after 24 h of treatment. These ratios represent the chance to obtain dead cells in a specific sample compared to the chance of obtaining dead cells in the respective correlated sample (Supplementary Information S13 and S14).

FAIK3-5 cells were treated with different concentrations of DMSO (0.4% (*v/v*) – 1.2% (*v/v*)) and the trolopone lacking compound **6**, as described before (Supplementary Table S3 and Supplementary Fig. S5). The results show a significant increase in dead cells in DMSO and 4-hydroxy norxenovulene B (**6**) treated samples compared to untreated controls, however, no dose-dependency was observed. The measured viability in all samples ranged from 91.7 % to 99.8 %, which lies within the measured range of cell viability for untreated cultures of FAIK3-5 cells (89.9

– 97 %) and is considerably higher than after treatment with the bistropolones pycnidione (**1**) (48.5 - 71.8 %) and eupenifeldin (**2**) (55.8 – 72.1 %) (Supplementary Table S3).

Comparing the effects of the different analysed compounds on cell survival, we observed a significant increase in the proportion of dead FAIK3-5 cells upon treatment with pycnidione (**1**) ($p < 0.001$), eupenifeldin (**2**) ($p < 0.001$), xenovulene B (**3**) ($p = 0.012$) and 4-hydroxyxenovulene B (**4**) ($p = 0.004$), compared to the untreated controls (Fig. 3). By analysing the effect on cell survival compared to the tropolone lacking compound 4-hydroxy norxenovulene B (**6**) instead of untreated samples, FAIK 3-5 cells exhibited a highly increased proportion of dead cells after treatment with the bistropolones **1** and **2** ($p < 0.001$), but not after treatment with the monotropolones **3, 4** and **5**. Thus, the inclusion of a second tropolone moiety to the TS-core structure seemed to have an additional effect on cell survival, emphasized by the significantly lower amount of detected dead cells in samples treated with xenovulene B (**3**) compared to pycnidione (**1**) ($p = 0.036$). The monotropolone 4-dehydroxy norpycnidione (**5**) showed no significantly enhanced cell death compared to untreated controls and samples treated with the tropolone-lacking compound 4-hydroxy norxenovulene B (**6**), indicating that cell toxicity to FAIK3-5 cells was significantly lower than for both bistropolones ($p \leq 0.001$, Fig. 3).

The results suggest that the presence of tropolone moieties on compounds significantly influences cell survival of FAIK3-5 cells, while increased cytotoxic effects were observed on dual-substituted compounds.

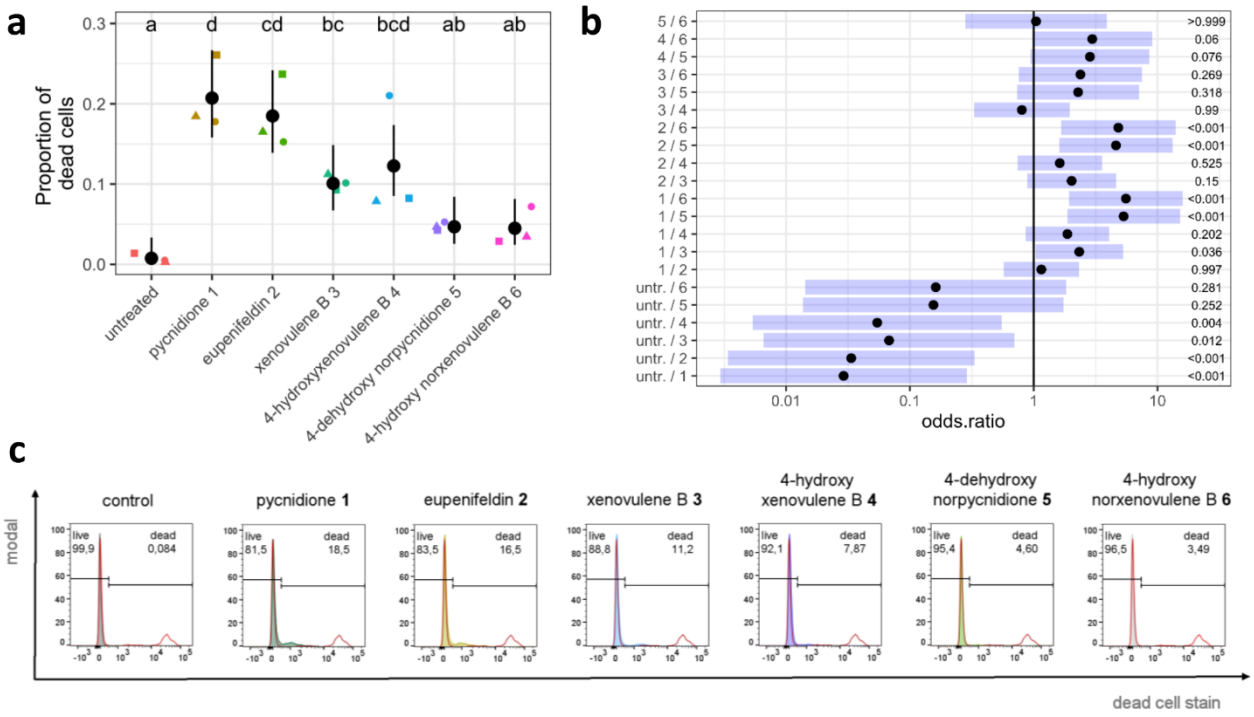

Figure 3: Cell viability of FAIK3-5 cells after treatment with pycnidione (**1**), eupenifeldin (**2**), xenovulene B (**3**), 4-hydroxyxenovulene B (**4**) and 4-dehydroxy norpycnidione (**5**) for 24 h and compared to untreated controls and tropolone moiety lacking compound 4-hydroxy norxenovulene B (**6**). Statistical analysis was conducted based on the calculation of the average proportion of dead cells per samples (samples size = 10.000 cells). **(a)** Proportions of dead cells (black dots) and their pointwise 95 % confidence intervals (error bars) of three biological replicates (● = 1, ▲ = 2, ■ = 3). Treatments marked with the same letter do not differ significantly from each other (α = 0.05). **(b)** Multiple comparisons of calculated odds ratios (black dots) and simultaneous 95 % confidence intervals (blue bars, details see Supplementary Information S14) showing differences of cell survival between samples treated with tropolone moiety containing compounds (**1** – **5**) compared to untreated samples or tropolone-lacking compound **6**. P-values for each contrast test of different treatments are displayed on the right side. **(c)** Representative plot of fluorescent intensities of SYTOX™ AADvanced™ stained FAIK3-5 cells samples. Each plot displays percentages of living and dead populations in an untreated control sample and after treatment with and the TS compounds pycnidione (**1**), eupenifeldin (**2**), xenovulene B (**3**) and 4-hydroxyxenovulene B (**4**) and 4-dehydroxy norpycnidione (**5**)**,** and tropolone lacking compound 4-hydroxy norxenovulene

B (**6**). Peaks of fluorescence intensities are displayed with the respective living / dead control (red) containing a heat-killed dead cell population.

Tropolone-sesquiterpenoid compounds do not enhance erythropoietin protein production in a cell model for natural EPO production

Epolone-dependent induction of erythropoietin reporter gene activity and protein expression has been observed in several cell lines [22,23], suggesting that specific TS compounds may influence EPO synthesis independently of oxygen availability. To assess if the utilized compounds can stimulate natural EPO production in REP-derived FAIK3-5 cells *in vitro*, EPO protein content was measured via ELISA.

Based on previous studies [22,23] and preliminary experiments (Supplementary Fig. S6), optimal compound concentrations for testing effects on EPO production was determined. In the following experiments pycnidione (**1**), eupenifeldin (**2**), xenovulene B (**3**), and 4-hydroxy norxenovulene B (**6**) were used at a concentration of 6 µM and 4-dehydroxy norpycnidione (**5**) was applied at 12 µM, where EPO production was higher in comparison to 6 µM. Treatment with different concentrations of 4-hydroxyxenovulene B (**4**) did not reveal a dose-dependent effect on EPO production in FAIK3-5 cells. However, as REP cells usually are quiescent or show little proliferation capacity [50,51] and due to the dose-dependent decrease in proliferation after 4-hydroxyxenovulene B (**4**) treatment (Supplementary Fig. S2), we also chose a concentration of 12 µM for subsequent studies on EPO production.

We found variability between biological replicates and no significant effect of the compounds on EPO protein production (Fig. 4 **a** and Supplementary Information S15). One possible reason could be epigenetic silencing of EPO synthesis by hypermethylation of EPO promoter and regulatory gene sequences [52]. To counteract this, samples were treated with 1 µM of the DNA

methyltransferase inhibitor 5-Azacytidine (5-Aza) for six days. As the vehicle control DMSO itself might support hypermethylation events within the cells [53], the effectiveness of 5-Aza treatment in enhancing EPO production of FAIK3-5 cells was assessed in DMSO vehicle controls (0.6% (*v/v*) and 1.2% (*v/v*)) that showed an increase in measured basic EPO concentrations (Fig. 4 **b**). However, additional treatment with TS compounds showed no enhancing effect on EPO protein synthesis after 5-Aza treatment compared to the respective vehicle controls (Fig. 4 **c**). Treatment with 4-hydroxyxenovulene B (**4**) ($p = 0.008$), 4-dehydroxy norpycnidione (**5**) ($p = 0.028$) and eupenifeldin (**2**) ($p = 0.046$) significantly decreased the measured EPO protein content compared to the vehicle control, yet, the effect of eupenifeldin (**2**) on 5-Aza treated FAIK3-5 cells was considered as marginal (Fig. 4 **d**).

Summing up, our results showed that the utilized TS compounds did not enhance EPO production in the REP cell line model, despite showing bioactivity in cell growth inhibition and cytotoxicity. Moreover, three out of six tested TS compounds, namely the bistropolones eupenifeldin (**2**), and the monotropolones 4-hydroxyxenovulene B (**4**) and 4-dehydroxy norpycnidione (**5**) significantly decreased EPO concentrations in 5-Aza treated FAIK3-5 cells. Thus, we found that the newly characterized 4-hydroxyxenovulene B (**4**) and 4-dehydroxy norpycnidione (**5**) compounds demonstrate versatile influences on cellular behaviour.

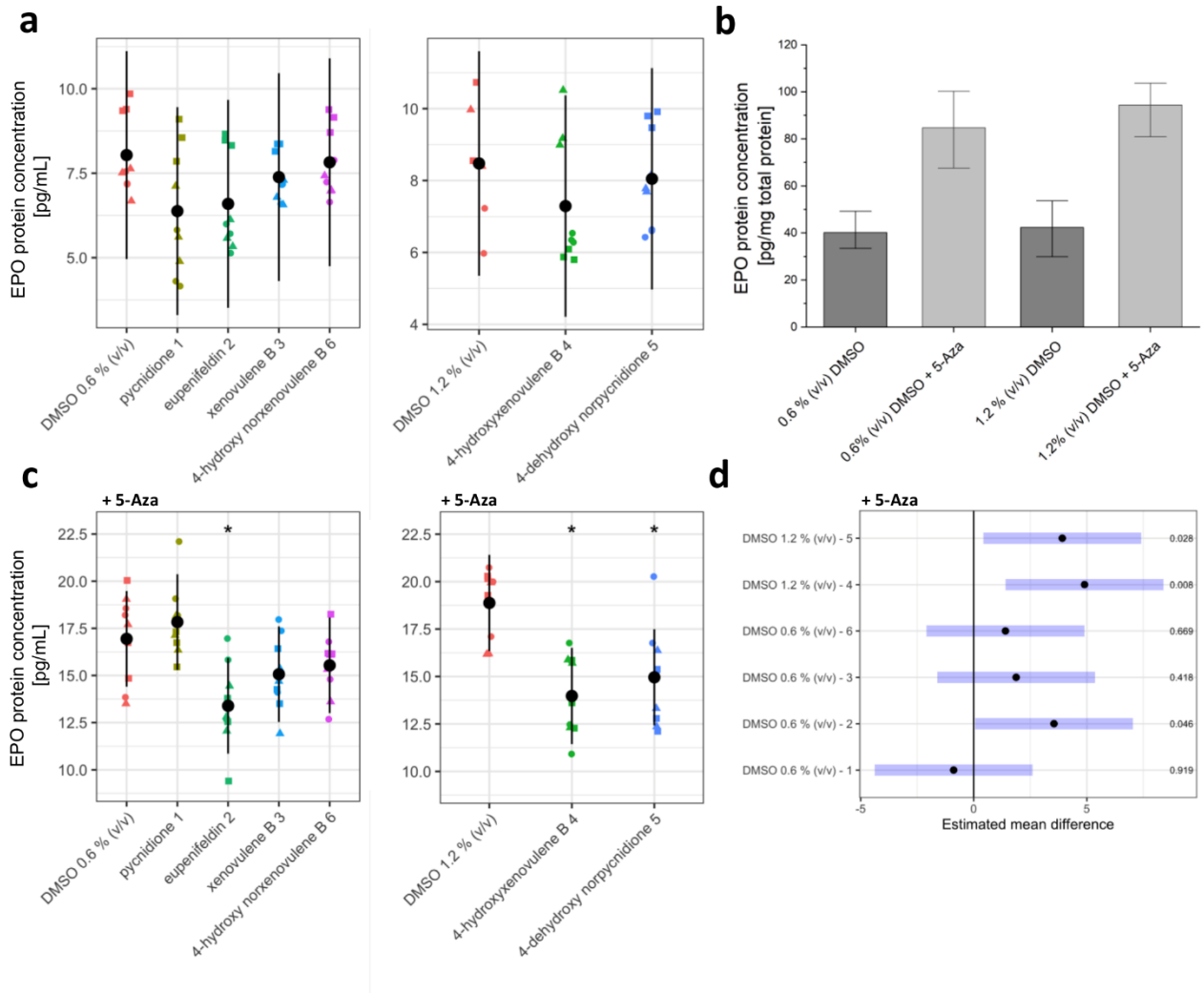

Figure 4: Erythropoietin (EPO) content of FAIK3-5 samples treated with the tropolone sesquiterpenoids (TS) pycnidione (**1**), eupenifeldin (**2**), xenovulene B (**3**), 4-hydroxyxenovulene B (**4**), 4-dehydroxy norpycnidione (**5**) and tropolone-lacking compound 4-hydroxy norxenovulene B (**6**) and their respective vehicle controls (DMSO 0.6% (*v/v*), DMSO 1.2 % (*v/v*)). **(a)** EPO protein concentrations measured in three biological replicates (● = 1,▲ = 2, ■ = 3) of FAIK3-5 cells treated with 6 µM of TS compounds **1**, **2**, **3**, tropolone- moiety lacking compound **6** and their respective DMSO vehicle control (0.6 % (*v/v*)) or 12 µM of TS compounds **4**, **5**, and their respective DMSO vehicle control (1.2 % (v/v)) without pre-treatment of 5-Azacytidine (5-Aza). Block dots are indicating the model based least square means and their pointwise 95% confidence intervals (black bars). **(b)** Measurement of basic EPO protein content in FAIK3-5 DMSO vehicle controls (0.6 % (*v/v*) and 1.2 % (*v/v*) with and without 5-Aza treatment for 6 days. Error bars

indicate the standard deviation of mean EPO concentrations. **(c)** EPO protein concentrations measured in three biological replicates (● = 1, ▲ = 2, ■ = 3) of FAIK3-5 cells treated with 6 µM of TS compounds **1**, **2**, **3**, tropolone- moiety lacking compound **6** and their respective DMSO vehicle control (0.6 % (*v/v*)), or 12 µM of TS compounds **4**, **5**, and their respective DMSO vehicle control (1.2 % (v/v)) with pre-treatment of 5-Azacytidine (+ 5-Aza). Block dots are indicating the model based least square means and their pointwise 95% confidence intervals (black bars). Treatments marked with ***** are significantly different from their respective vehicle controls. **(d)** Pairwise mean comparisons showed significant differences in EPO protein concentrations 4-hydroxyxenovulene B (**4**), 4-dehydroxy norpycnidione (**5**) and eupenifeldin (**2**) compared to their respective vehicle controls. Black dots indicate back transformed means of measured EPO concentrations and their 95% confidence intervals (blue bars). Respective p-values for each calculation are displayed on the right side. The estimated contrasts and corresponding confidence intervals are given in the Supplementary Information S16.

DISCUSSION

This study examines the impact of TS compound treatment on murine REP-derived cells, focusing on the relationship between their molecular structures and observed biological effects. Here, we report the first bioactivities for xenovulene B (**3**), 4-hydroxyxenovulene B (**4**) and 4-dehydroxy norpycnidione (**5**). Moreover, we found that the bioactivities of the tested TS compounds, particularly cytotoxicity and growth inhibition, are strongly dependent on the tropolone proportions used. We observed that the bistropolones pycnidione (**1**) and eupenifeldin (**2**) showed significantly higher cytotoxic potency than the monotropolones xenovulene B (**3**) and 4-hydroxyxenovulene B (**4**). Monotropolones like xenovulene B (**3**) and 4-hydroxyxenovulene B (**4**) or sesquiterpene phenols like 4-dehydroxy norpycnidione (**5**) were less potent, and the tropolone lacking compound 4-hydroxy norxenovulene B (**6**) was even unable to cause biological reactions in the tested cells. The results support previous research showing that methylated pycnidione derivatives are inactive in causing EPO gene expression in hepatic cell lines [22] and

enhancing bleomycin treatment effects in Jurkat cells [18]. This suggests that the number of unprotected tropolone moieties is crucial for TS potency, although the exact structure-activity relationship remains unclear.

Previous reports of EPO induction by TS compounds of the "epolone family" in reporter cell lines of Hep3B [22], HepG2, and HRCHO5 [23] led to the hypothesis that certain TS compounds might play a role in the induction of EPO synthesis independent of oxygen availability, *e.g.* by inhibiting proteins containing a HIF-prolyl hydroxylase domain. To better match physiological conditions, the nonconditionally immortalized murine REP-dervied cell line FAIK3-5 [37] was chosen as a model for natural EPO production *in vitro*. For these cells TS treatment showed no enhancement of EPO production. However, previous reports were based on indirect measurements of EPO gene induction or performed on genetically engineered cancer cell lines, which may have less accounted for cell-type specific and transcriptional regulation of EPO expression. EPO production is tightly regulated at the transcriptional level, with DNA methylation of the EPO promoter partially involved in epigenetic inactivation of EPO expression [54]. This mechanism was also previously observed in the utilized REP cell line and the authors proposed the occurrence of an intrinsic transcriptional negative feedback loop responsible for the decline in EPO production upon longer cultivation periods [37]. Additionally, despite its universal use in cryopreservation or as a solvent for poorly soluble molecules, there is evidence of DMSO toxicity at low doses and its impacts on the epigenetic landscape of treated samples [53,55], which may have further implications on protein expression after treatment. Correspondingly, we observed significant effects of DMSO on proliferation and cell viability, although the observed inhibition of cell growth and cytotoxicity were considerably lower than in samples treated with TS compound **1** – **5** or did not show a dose-response relationship.

To circumvent the effects of DNA methylation of the EPO-regulatory loci or the *Epo* locus itself, the cell line was treated with the DNA methyltransferase inhibitor 5-Aza for six days prior to TS compound treatment. We found an increase in basic EPO production compared to samples with putative regulatory methylation, but no significant enhancement after TS treatment compared to vehicle controls, leading to the assumption that the complex epigenetic regulation has a major impact on protein synthesis *in vitro*. Since EPO-producing cells are in a quiescent state *in vivo* [51], it is possible that this specific stage is required for normal oxygen sensing and signaling in cultured FAIK3-5 cells. We found that the addition of eupenifeldin (**2**), 4-hydroxyxenuvolene B (**4**), or 4-dehydroxy norpycnidione (**5**) to 5-Aza treated cells led to a significant decrease in basic EPO production compared to vehicle controls. However, there was no direct correlation between the molecular structures of the compounds and the number of tropolone substitutions. Treatment with eupenifeldin (**2**) also resulted in lower cell survival compared to untreated control samples, and cells treated with tropolone-lacking compound 4-hydroxy norxenovulene B (**6**) and TS compound 4-dehydroxy norpycnidione (**5**)**,** which may explain the low protein concentration in these samples. Since we observed significant inhibition of proliferation by all studied tropolone-bearing TS compounds (**1**-**5**), the observed effects on cellular EPO content in 4-hydroxyxenuvolene B (**4**) or 4-dehydroxy norpycnidione (**5**) treated samples cannot be exclusively due to decreased total protein expression caused by low cellular metabolism. The study focuses on the measurement of EPO protein concentration without relying on indirect protein measurement methods like firefly luciferase reporter assays. These assays are widely used in molecular biology and high-throughput screening for small molecules [56], but can lead to biased signal output due to false-positive results. In particular, the counterintuitive phenomenon of signal activation by luciferase inhibitor molecules can increase signal strength indistinguishable from transcriptional

activation of the reporter gene [57]. This effect has been reported for other bioactive compounds like sesquiterpene lactones, which inhibit luciferase activity probably by directly targeting the enzyme [58]. Thompson et al. reported that measured luciferase activities increased up to 20-fold in a concentration-dependent manner after adding potent luciferase inhibitors like PBT or HPBT to HepG2 cell culture medium [59]. The study suggests that the described EPO-enhancing properties of reported epolone compounds need to be reevaluated, and the need for careful investigation of possible interference of TS compounds with firefly luciferase-based drug screening assays is highlighted.

Apart from their effect on protein expression, the treatment of TS compounds resulted in a strong inhibition of cell proliferation and morphological alteration in our model. The monotropolone compound 4-dehydroxy norpycnidione (**5**) showed a significantly improved proliferation inhibition compared to the tropolone-lacking compound 4-hydroxy norxenovulene B (**6**) and untreated control samples. However, at the same time cytotoxic effects exerted on the model cell line were significantly lower than those of pycnidione (**1**) or eupenifeldin (**2**). The reduced toxicity and concomitant severe growth retardation induced by 4-dehydroxy norpycnidione (**5**) could be a sign of cell transition to a senescent stage. In addition to cell growth discontinuation, alterations of cell morphology can also reflect senescent cell stages *in vitro* by the emergence of an enlarged, flat and multinucleated phenotype which is highly granulated [60]. We observed severe morphological alterations in FAIK3-5 cells treated with different TS compounds, with 4-hydroxyxenovulene B (**4**) showing the largest measured cell area compared to other treatments. The occurrence of large and highly granulated cells was visible in all treated samples. Related chemical compounds such as pycnidione (**1**) and eupenifeldin (**2**), as well as xenovulene B (**3**), and 4-hydroxyxenovulene B (**4**) induced similar phenotypic alteration in treated FAIK3-5 cells,

suggesting that the compounds likely target similar biological pathways via specific receptors, leading to the same biological responses reflected in cell morphology. Brandhagen et al. observed that mifepristone-induced cytostasis in ovary cancer cell lines resulted in morphological changes, with cells developing a thin cytoplasm and neurite-like protrusions [61], similar to the observed morphological changes in cells treated with bistropolones pycnidione (**1**) or eupenifeldin (**2**). Assuming different types of senescence observed *in vitro* and induced by different stimuli [62], it is possible that some of the used TS compounds could have promoted senescence in FAIK3-5 samples despite the morphological differences between them. *In vitro* senescence is defined as irreversible loss proliferative potential of cells, distinguishing it from reversible non-senescent growth arrest such as cellular quiescence [63]. Therefore, in our study, the observed significant proliferation inhibition could be caused by both processes. However, considering that the bistropolone pycnidione (**1**) has already been described as inducing cell cycle arrest and, moreover, enhancing bleomycin cytotoxicity in Jurkat cells [18,19], we might expect a similar mode of action of the related bioactive TS compounds, making them interesting targets for subsequent clinical studies.

This study reveals the bioactive properties of xenovulene B (**3**), 4-hydroxyxenovulene B (**4**), and 4-dehydroxy norpycnidione (**5**), showing a significant relationship between tropolone substitutions and cell viability. Eupenifeldin (**2**), 4-hydroxyxenovulene B (**4**) and 4-dehydroxy norpycnidione (**5**) show versatile effects on cellular behavior and reduce EPO content in hypomethylated FAIK3-5 cells. 4-dehydroxy norpycnidione (**5**) additionally exhibit high proliferative inhibition and low cytotoxic effects, making it a potential compound for pre-clinical drug testing for cancer treatment.

METHODS

Biosynthesis of tropolone-sesquiterpenoid compounds

Pycnidione **1** and eupenifeldin **2** were isolated respectively from *Leptobacillium* sp. CF-236968 and *Phaeosphaeriaceae* sp. CF-150626 (formerly referred to as unidentified ascomycete F-150626) that naturally produce the compounds, as reported in Schotte et al (Schotte et al. 2020). For the heterologous production of the described tropolone sesquiterpenoid (TS) compounds **3-5** and control compound 4-hydroxy norxenovulene B **6**, a series of TS key biosynthetic gene clusters (BGC) were refactored and recombined in *A. oryzae* NSAR1 as previously described by Schotte et. al [31]. The currently accepted stereochemistry of these compounds is displayed in Fig. 5 [32].

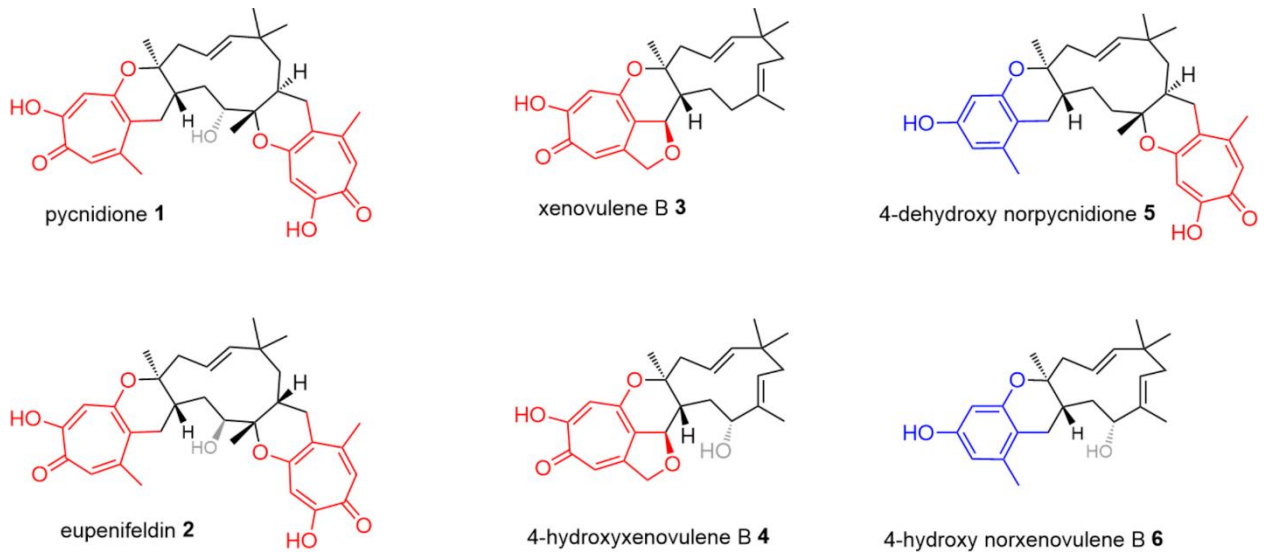

Figure 5: Stereochemistry of selected tropolone sesquiterpene (TS) compounds (**1**-**5**) and control compound (**6**) lacking a tropolone moiety [32]. Key features are highlighted in red (= polyketide derived tropolones), blue (= benzopyranyl moiety) and grey (C-10 hydroxylation).

Cell culture of fibroblastoid interstitial kidney (FAIK) 3-5 cells

Fibroblastoid atypical interstitial kidney (FAIK) 3-5 cells were obtained from the Leibniz Institute DSMZ-German Collection of Microorganisms and Cell Cultures GmbH (Braunschweig, Germany) and were cultured according to the recommended culturing protocol in Dulbecco′s Modified Eagle′s Medium (DMEM) - high Glucose (Sigma Aldrich, St. Louis, MO, United States) supplemented with 10 % FBS (Sigma Aldrich, St. Louis, MO, United States; Lot: BCBW9923), which is referred to in the following as cell culture medium. As the cell line was previously described to produce EPO protein for at least 30 passages [37], all experiments were conducted on cells below that passage number. Cells were split every two to three days and at a confluency of 80 – 90 %.

Compound reconstitution and TS treatment of FAIK3-5 cells

Lyophilized TS compounds were reconstituted in dimethylsulfoxid (DMSO, Carl Roth GmbH, Karlsruhe, Germany) to obtain 1 mM stock solutions, sterile filtered and stored at -20 °C until further use. To maintain compound stability, repeated freeze-thaw cycles of compound aliquots were avoided. For the investigation of TS compound influence on FAIK3-5 cells, 5×10^5 cells / well (6well, CellStar™, Greiner Bio-One, Kremsmünster, AT) were seeded and kept in culture for 24 h, before cell adherence and morphology were assessed visually. Prior to TS treatment FAIK3-5 cells were washed thoroughly with Dulbecco's Phosphate Buffered Saline (DPBS) (Sigma Aldrich, St. Louis, MO, United States) and incubated with 4-12 µM TS compound containing cell culture media for another 24 h. For subsequent experiments with compound treated cells, respective DMSO vehicle controls and untreated medium controls were used.

For the determination of EPO concentrations FAIK3-5 cells were treated with TS compounds, respective vehicle controls (0.6 % *v/v* and 1.2 % *v/v* DMSO) or not treated for 24 h as described above and cell extracts were analysed for EPO protein concentrations. It is known that the physiological EPO production is tightly controlled by an "on-off" regulatory behaviour of REP cells and by DNA methylation in the *EPO*-gene promoter that can cause the loss of EPO production capability in REP cells [52]. Therefore, FAIK3-5 were treated with 1 µM of the hypomethylating agent 5-Azacytidine (5-Aza, Sigma-Aldrich, St. Louis, MO, United States) in an additional approach. The treatment was conducted for six days with complete medium changes every other day to ensure sufficient cell divisions for 5-Aza integration and agent replenishment before degradation. After this period the cells were treated with TS compounds and vehicle controls (0.6 % *v/v* and 1.2 % *v/v* DMSO) and EPO protein content was measured.

Morphological analysis

In order to handle environmental changes, cells possess the ability to attain a more desirable stress state by the activation of distinct molecular pathways, which morphologically might lead to profound changes of cell shapes. To analyse different morphological shapes of FAIK3-5 cells caused by TS compound treatment, brightfield pictures were taken with a ZEISS Axio Vert.A1 Inverted Microscope (Zeiss, Oberkochen, Germany) 24 h after TS treatment and directly before subsequent analysis of the cells.

For each treatment condition at least 20 cells from three independent experiments were analysed for morphological changes with Fiji (ImageJ, Version 1.53c bundled with Java 1.8.0_172) [64]. The results were visualized using OriginPro 2021 (Version 9.8.0.200) and the Matlab (Version R2021b) toolbox PhenoPlot [47], an open source visualization tool for imaging data that is able to

represent multiple dimensions of cellular morphology as intuitive cell-like glyphs. To obtain the most accurate illustration of different cell shapes, regions of interest (ROIs) were drawn by hand and basic morphometric variables (cell area, perimeter, major and minor axis) and standard shape descriptors (circularity, aspect ratio, roundness and solidity) were measured in Fiji. To analyse differences in ramification patterns of cells treated with distinct TS compounds two-dimensional branching descriptors were calculated using the AnalyzeSkeleton plugin [43]. For a detailed description of morphological analysis and PhenoPlot visualization see Supplementary Fig. S7.

Proliferation and Cytotoxicity Assay

To evaluate effects of proliferative behaviour and cell viability caused by TS compounds, FAIK3-5 cells were cultured in cell culture medium as described above and labelled with the CellTrace™ Violet (CTV) Cell Proliferation Kit (Invitrogen, ThermoFisher Scientific, Waltham, MA, United States) at a concentration of 10 µM CTV per 1×10^6 cells according to the manufacturer's protocol with minor modifications. To assure homogenous CTV labelling, 900 µl of cell suspension containing 1×10^6 cells were kept in a 15 mL tube (Greiner Bio-One, Kremsmünster, Austria), which was positioned horizontally before 100 µl of CTV staining solution was added to the upper end of the tube without mixing. The tube was kept in that position until the lid was closed carefully, and mixing was conducted on a vortex mixer (Benchmark Scientific, Sayreville, NJ, United States). After 20 minutes of staining at 37 ° C in the dark, the reaction was stopped by adding 5 times the original staining volume of DPBS with 10 % of FBS and incubation for 5 minutes on ice to remove unbound dye particles. Subsequently, the supernatant staining solution was removed after centrifugation at 300 × g for 5 minutes, and FAIK3-5 cells were counted and seeded into 6-well plates (Greiner Bio-One, Kremsmünster,

Austria) with a cell density of 5×10^5 cells per well. Cell viability was evaluated via SYTOX™ AADvanced™ Dead Cell Stain Kit (Invitrogen, ThermoFisher Scientific, Waltham, MA, United States) staining according to the manufacturer's instructions prior to analysis with the BD FACSverse™ Cell Analyzer (BD, Franklin Lakes, NJ, United States) cytometer.

Directly after staining, cell samples were analysed with the flow cytometer to ensure homogenous dye distribution within the population and to monitor cell viability after the staining process. For each analysed sample 10 000 events were counted. Gating strategies for living/dead discrimination and proliferation analysis are explained in more detail in the Supporting Information section (Supplementary Fig. S8). For each analysis unstained cells, CTV-stained cells without compound treatment and live/dead control samples, comprising a heat-killed population to set the fluorescence threshold for live/dead discrimination, were included as staining controls. To assess the optimal analysis period for the CTV proliferation tests, untreated FAIK3-5 cells were analysed via flow cytometry for CTV intensities and putative effects of the CTV staining on cell viability on three subsequent days in preliminary experiments (Supplementary Fig. S8).

For following experiments with compound treated samples, measurements were taken at day 1 (d1) to obtain the basic CTV intensities of the stained samples. At day 2 TS compound treatment was started and at day 3 (d3), after 24 h of incubation, the second measurement was conducted to evaluate changes in CTV intensities after TS treatment. For each experiment untreated cells and vehicle controls (0.6 % v/v and 1.2 % v/v DMSO) were included as treatment control samples. After cellular uptake by diffusion, CTV covalently binds to intracellular amines and is diluted proliferation dependently within the analysed cellular populations. However, as the cellular uptake and binding capacity is contingent on multiple factors (e.g. cell viability, division stage or cellular protein level), a perfectly homogenous staining throughout experimental repetitions is not possible

and hence result in distinct MFIs at d1 of the experiments. Accordingly, for statistical analysis obtained values were normalized by calculating the proportions of measured MFIs at the beginning (d1) and end (d3) of the experiments and pairwise mean comparison tests were run based on mean differences. For descriptive statistics mean values and standard deviations were obtained from the calculated fold changes enlisted in Supplementary Table S3.

Analysis of erythropoietin production via Enzyme-linked Immunosorbent Assay

In previous studies an enhancing effect on the EPO production of pycnidiones and structurally related epolones was described for Hep3B and HRCHO5 reporter cell lines [22,23]. To analyse, if the utilized compounds are also capable to induce a similar effect on the natural EPO production of REP-derived FAIK3-5 cells *in vitro*, the EPO protein content of TS compound treated FAIK3-5 derived cell extracts was measured via enzyme-linked immunosorbent (ELISA) assays, using the RayBio® Mouse EPO ELISA Kit (Raybiotech, Peachtree Corners, GA, United States) according to the manufacturer's protocol.

Cell Extracts were obtained from either untreated, TS treated samples or vehicle controls cultured as described above. After visual examination of growth density, cells were washed twice in ice-cold DPBS and disrupted in RIPA buffer (ThermoFisher Scientific, Waltham, MA, United States) supplemented with SIGMAFAST™ Protease Inhibitor Tablets (Sigma Aldrich, St. Louis, MO, United States) to prevent protein degradation. Samples were stored at -80 °C or directly used for the quantification of total protein concentrations with the Pierce™ BCA Protein Assay Kit (ThermoFisher Scientific, Waltham, MA, United States). Thereafter, samples were diluted to a total protein concentration of 200 µg/mL and murine EPO ELISA analysis was conducted. Finally, absorbance at 450 nm was measured immediately with the Infinite Mono 200 Platereader (Tecan,

Männedorf, Switzerland) and experiments were analysed with the provided Excel based freeware ELISA analysis tool v1.0 (Raybiotech, Peachtree Corners, GA, United States).

Statistical analysis

The statistical analysis was done based on R version 4.2.1 [65] on a 2021 MacBook Pro using the aarch64-apple-darwin20 (64-bit) platform. Data management and plotting was done using the tidyverse packages [66]. Depending on the scale of the endpoints and the experimental design, linear models, generalized linear models or linear mixed models were fit to the data. Linear and generalized liner models were fit using the lm() and glm() functions from the stats package [65]. Mixed effects models were fitted using lmer() from the lme4 package [67]. Based on the fitted models either an ANOVA (for linear models) or an analysis of deviance (for generalized linear models) was run. For each of the fitted mixed effects models, a type III ANOVA was computed using Kenward-Roger´s approximation of degrees of freedom [68]. Subsequently, mean comparisons were done using the packages emmeans [69] and multcomp [70]. Since the endpoints regarding the cell morphology are highly correlated (several endpoints per cell), multiple comparisons were done based on the multiple marginal model approach [45,46]. Together with the data and the R code, a detailed description of the statistical methodology is given in the Supplementary Information (S9 - S16).

DATA AVAILABILITY STATEMENT

All data generated or analysed during this study are included in this published article (and its Supplementary Information files) or are available from the corresponding author on reasonable request.

References

1. Peláez, F. in *Handbook of industrial mycology,* edited by Z. An (M. Dekker, 2005), pp. 49–92.
2. Schueffler, A. & Anke, T. Fungal natural products in research and development. *Natural product reports* **31,** 1425–1448 (2014).
3. Choy, K. W., Murugan, D. & Mustafa, M. R. Natural products targeting ER stress pathway for the treatment of cardiovascular diseases. *Pharmacological research* **132,** 119–129 (2018).
4. Langeder, J. *et al.* Natural products against acute respiratory infections: Strategies and lessons learned. *Journal of Ethnopharmacology* **248,** 112298 (2020).
5. Yu, S., Liu, M. & Hu, K. Natural products: Potential therapeutic agents in multiple sclerosis. *International immunopharmacology* **67,** 87–97 (2019).
6. Essa, M. M., Akbar, M. & Guillemin, G. *The Benefits of Natural Products for Neurodegenerative Diseases* (Springer International Publishing; Imprint; Springer, 2016).
7. Demain, A. L. & Vaishnav, P. Natural products for cancer chemotherapy. *Microbial biotechnology* **4,** 687–699 (2011).
8. Cragg, G. M., Grothaus, P. G. & Newman, D. J. Impact of natural products on developing new anti-cancer agents. *Chemical reviews* **109,** 3012–3043 (2009).
9. Abdelmohsen, U. R. *et al.* Potential of marine natural products against drug-resistant fungal, viral, and parasitic infections. *The Lancet Infectious Diseases* **17,** e30-e41 (2017).
10. Hemaiswarya, S., Kruthiventi, A. K. & Doble, M. Synergism between natural products and antibiotics against infectious diseases. *Phytomedicine : international journal of phytotherapy and phytopharmacology* **15,** 639–652 (2008).

11. van Santen, J. A. *et al.* The Natural Products Atlas 2.0: a database of microbially-derived natural products. *Nucleic acids research* **50,** D1317-D1323 (2022).
12. Keller, N. P. Fungal secondary metabolism: regulation, function and drug discovery. *Nature reviews. Microbiology* **17,** 167–180 (2019).
13. Harris, G. H. *et al.* Isolation and structure determination of pycnidione, A novel bistropolone stromelysin inhibitor from a Phoma sp. *Tetrahedron* **49,** 2139–2144 (1993).
14. Mayerl, F. *et al.* Eupenifeldin, a novel cytotoxic bistropolone from Eupenicillium brefeldianum. *J. Antibiot.* **46,** 1082–1088 (1993).
15. Bunyapaiboonsri, T., Veeranondha, S., Boonruangprapa, T. & Somrithipol, S. Ramiferin, a bisphenol-sesquiterpene from the fungus Kionochaeta ramifera BCC 7585. *Phytochemistry Letters* **1,** 204–206 (2008).
16. Al Subeh, Z. Y. *et al.* Delivery of eupenifeldin via polymer-coated surgical buttresses prevents local lung cancer recurrence. *Journal of controlled release : official journal of the Controlled Release Society* **331,** 260–269 (2021).
17. Pittayakhajonwut, P. *et al.* Pughiinin A, a Sesquiterpene from the Fungus Kionochaeta pughii BCC 3878. *Planta Med* **68,** 1017–1019 (2002).
18. Kaneko, M. *et al.* Potentiation of bleomycin in Jurkat cells by fungal pycnidione. *Biological & pharmaceutical bulletin* **35,** 18–28 (2012).
19. Hsiao, C.-J. *et al.* Pycnidione, a fungus-derived agent, induces cell cycle arrest and apoptosis in A549 human lung cancer cells. *Chemico-biological interactions* **197,** 23–30 (2012).
20. Höller, U. *et al.* Fungi from marine sponges: diversity, biological activity and secondary metabolites. *Mycological Research* **104,** 1354–1365 (2000).

21. Wright, A. D. & Lang-Unnasch, N. Potential antimalarial lead structures from fungi of marine origin. *Planta medica* **71,** 964–966 (2005).

22. Cai, P. *et al.* Epolones: novel sesquiterpene-tropolones from fungus OS-F69284 that induce erythropoietin in human cells. *Journal of natural products* **61,** 791–795 (1998).

23. Wanner, R. M. *et al.* Epolones induce erythropoietin expression via hypoxia-inducible factor-1 alpha activation. *Blood* **96,** 1558–1565 (2000).

24. Chen, S. *et al.* Phomeroids A and B: two novel cytotoxic meroterpenoids from the deep-sea-derived fungus Phomopsis tersa FS441. *Org. Chem. Front.* **7,** 557–562 (2020).

25. El-Elimat, T. *et al.* Meroterpenoids from Neosetophoma sp.: A Dioxa4.3.3propellane Ring System, Potent Cytotoxicity, and Prolific Expression. *Organic letters* **21,** 529–534 (2019).

26. Bunyapaiboonsri, T., Veeranondha, S., Boonruangprapa, T. & Somrithipol, S. [Copy] Ramiferin, a bisphenol-sesquiterpene from the fungus Kionochaeta ramifera BCC 7585. *Phytochemistry Letters* **1,** 204–206 (2008).

27. Pittayakhajonwut, P. *et al.* [Copy] Pughiinin A, a Sesquiterpene from the Fungus Kionochaeta pughii BCC 3878. *Planta Med* **68,** 1017–1019 (2002).

28. Ainsworth, A. M. *et al.* Xenovulene A, a novel GABA-benzodiazepine receptor binding compound produced by Acremonium strictum. *The Journal of Antibiotics* **48,** 568–573 (1995).

29. Raggatt, M. E., Simpson, T. J. & Inês Chicarelli-Robinson, M. Biosynthesis of Xenovulene A®: formation of a cyclopentenone via a unique ring expansion–ring contraction mechanism. *Chem. Commun.,* 2245–2247 (1997).

30. Schor, R., Schotte, C., Wibberg, D., Kalinowski, J. & Cox, R. J. Three previously unrecognised classes of biosynthetic enzymes revealed during the production of xenovulene A. *Nat Commun* **9,** 1963 (2018).

31. Schotte, C., Li, L., Wibberg, D., Kalinowski, J. & Cox, R. J. Synthetic Biology Driven Biosynthesis of Unnatural Tropolone Sesquiterpenoids. *Angewandte Chemie (International ed. in English)* **59,** 23870–23878 (2020).

32. Li, L. & Cox, R. J. Stereochemical and Biosynthetic Rationalisation of the Tropolone Sesquiterpenoids. *Journal of fungi (Basel, Switzerland)* **8** (2022).

33. Bemis, C. Y. *et al.* Total Synthesis and Computational Investigations of Sesquiterpene-Tropolones Ameliorate Stereochemical Inconsistencies and Resolve an Ambiguous Biosynthetic Relationship. *Journal of the American Chemical Society* **143,** 6006–6017 (2021).

34. Rokas, A., Mead, M. E., Steenwyk, J. L., Raja, H. A. & Oberlies, N. H. Biosynthetic gene clusters and the evolution of fungal chemodiversity. *Natural product reports* **37,** 868–878 (2020).

35. Yang, Z.-Y., He, J.-H., Lu, A.-P., Hou, T.-J. & Cao, D.-S. Frequent hitters: nuisance artifacts in high-throughput screening. *Drug discovery today* **25,** 657–667 (2020).

36. Obara, N. *et al.* Repression via the GATA box is essential for tissue-specific erythropoietin gene expression. *Blood* **111,** 5223–5232 (2008).

37. Imeri, F. *et al.* Generation of renal Epo-producing cell lines by conditional gene tagging reveals rapid HIF-2 driven Epo kinetics, cell autonomous feedback regulation, and a telocyte phenotype. *Kidney international* **95,** 375–387 (2019).

38. Ziegler, S., Sievers, S. & Waldmann, H. Morphological profiling of small molecules. *Cell chemical biology* **28,** 300–319 (2021).

39. Xiong, Y. & Iglesias, P. A. Tools for analyzing cell shape changes during chemotaxis. *Integrative biology : quantitative biosciences from nano to macro* **2,** 561–567 (2010).

40. Chen, C. S., Mrksich, M., Huang, S., Whitesides, G. M. & Ingber, D. E. Geometric control of cell life and death. *Science (New York, N.Y.)* **276,** 1425–1428 (1997).

41. Watson, P. A. Function follows form: generation of intracellular signals by cell deformation. *FASEB journal : official publication of the Federation of American Societies for Experimental Biology* **5,** 2013–2019 (1991).

42. Lobo, J., See, E. Y.-S., Biggs, M. & Pandit, A. An insight into morphometric descriptors of cell shape that pertain to regenerative medicine. *Journal of tissue engineering and regenerative medicine* **10,** 539–553 (2016).

43. Arganda-Carreras, I., Fernández-González, R., Muñoz-Barrutia, A. & Ortiz-De-Solorzano, C. 3D reconstruction of histological sections: Application to mammary gland tissue. *Microscopy research and technique* **73,** 1019–1029 (2010).

44. Heisler, J. *et al.* Morphological Effects of Natural Products on Schizosaccharomyces pombe Measured by Imaging Flow Cytometry. *Natural products and bioprospecting* **4,** 27–35 (2014).

45. Pipper, C. B., Ritz, C. & Bisgaard, H. A versatile method for confirmatory evaluation of the effects of a covariate in multiple models. *Journal of the Royal Statistical Society: Series C (Applied Statistics)* **61,** 315–326 (2012).

46. Schaarschmidt, F. & Ritz C. Tukeytrend: tukeys trend test via multiple marginal models. R package version 0.7. *https://CRAN.R-project.org/package=tukeytrend* (2020).

47. Sailem, H. Z., Sero, J. E. & Bakal, C. Visualizing cellular imaging data using PhenoPlot. *Nat Commun* **6,** 5825 (2015).

48. Doncel, J. P. *et al. in Cytoskeleton - Structure, Dynamics, Function and Disease,* edited by J. C. Jimenez-Lopez (IntechOpen, 2017).

49. Farshori, N. N. *et al.* Aloe vera-induced apoptotic cell death through ROS generation, cell cycle arrest, and DNA damage in human breast cancer cells. *Biologia*; 10.1007/s11756-022-01124-5 (2022).

50. Dahl, S. L. *et al.* Fate-mapping of erythropoietin-producing cells in mouse models of hypoxaemia and renal tissue remodelling reveals repeated recruitment and persistent functionality. *Acta Physiologica (Oxford, England)* **234,** e13768 (2022).

51. Souma, T. *et al.* Plasticity of renal erythropoietin-producing cells governs fibrosis. *Journal of the American Society of Nephrology : JASN* **24,** 1599–1616 (2013).

52. Chang, Y.-T. *et al.* DNA methyltransferase inhibition restores erythropoietin production in fibrotic murine kidneys. *The Journal of clinical investigation* **126,** 721–731 (2016).

53. Verheijen, M. *et al.* DMSO induces drastic changes in human cellular processes and epigenetic landscape in vitro. *Scientific reports* **9,** 4641 (2019).

54. Sato, K. *et al.* An immortalized cell line derived from renal erythropoietin-producing (REP) cells demonstrates their potential to transform into myofibroblasts. *Scientific reports* **9,** 11254 (2019).

55. Galvao, J. *et al.* Unexpected low-dose toxicity of the universal solvent DMSO. *FASEB journal : official publication of the Federation of American Societies for Experimental Biology* **28,** 1317–1330 (2014).

56. Thorne, N., Inglese, J. & Auld, D. S. Illuminating insights into firefly luciferase and other bioluminescent reporters used in chemical biology. *Chemistry & biology* **17,** 646–657 (2010).

57. Auld, D. S., Thorne, N., Nguyen, D.-T. & Inglese, J. A specific mechanism for nonspecific activation in reporter-gene assays. *ACS chemical biology* **3,** 463–470 (2008).

58. Lindenmeyer, M. T., García-Piñeres, A. J., Castro, V. & Merfort, I. Sesquiterpene lactones inhibit luciferase but not beta-galactosidase activity in vitro and ex vivo. *Analytical Biochemistry* **328,** 147–154 (2004).

59. Thompson, J. F., Hayes, L. S. & Lloyd, D. B. Modulation of firefly luciferase stability and impact on studies of gene regulation. *Gene* **103,** 171–177 (1991).

60. Beck, J., Horikawa, I. & Harris, C. Cellular Senescence: Mechanisms, Morphology, and Mouse Models. *Veterinary pathology* **57,** 747–757 (2020).

61. Brandhagen, B. N. *et al.* Cytostasis and morphological changes induced by mifepristone in human metastatic cancer cells involve cytoskeletal filamentous actin reorganization and impairment of cell adhesion dynamics. *BMC cancer* **13,** 35 (2013).

62. Kuilman, T., Michaloglou, C., Mooi, W. J. & Peeper, D. S. The essence of senescence. *Genes & development* **24,** 2463–2479 (2010).

63. Terzi, M. Y., Izmirli, M. & Gogebakan, B. The cell fate: senescence or quiescence. *Molecular biology reports* **43,** 1213–1220 (2016).

64. Schindelin, J. *et al.* Fiji: an open-source platform for biological-image analysis. *Nature methods* **9,** 676–682 (2012).

65. R Core Team. R: A language and environment for statistical computing. R Foundation for Statistical Computing, Vienna, Austria. *http://www.R-project.org* (2022).

66. Wickham, H. *et al.* Welcome to the Tidyverse. *JOSS* **4,** 1686 (2019).

67. Bates, D., Mächler, M., Bolker, B. & Walker, S. Fitting Linear Mixed-Effects Models Using lme4. *J. Stat. Soft.* **67** (2015).

68. Kuznetsova, A., Brockhoff, P. B. & Christensen, R. H. B. lmerTest Package: Tests in Linear Mixed Effects Models. *J. Stat. Soft.* **82** (2017).

69. Lenth, R. V. emmeans: estimated marginal means, aka least-squares means. R package version 1.4. 7. 2020 . *https://CRAN.R-project.org/package=emmeans* (2022).

70. Hothorn, T., Bretz, F. & Westfall, P. Simultaneous inference in general parametric models. *Biometrical Journal* **50,** 346–363 (2008).

ACKNOWLEDGMENT

We would like to thank Frank Schaarschmidt for his valuable input and support in the biostatistics analysis of the experiments.

AUTHOR CONTRIBUTIONS

T.C.B.: Investigation (lead), Methodology (lead), Formal Analysis (equal), Visualization (lead), Writing – original draft (lead). M.M.: Formal Analysis (lead), Visualization (equal), Writing – Review and Editing (equal). C.S.: Resources (lead), Writing – Review and Editing (equal). R.J.C.: Conceptualization (equal), Resources (equal), Writing – Review and Editing (equal). C.L.T.: Conceptualization (lead), Funding Acquisition (lead), Project Administration (lead), Supervision (lead), Writing – Review and Editing (lead)

ADDITIONAL INFORMATION

Funding Sources

This work has been carried out within the framework of the SMART BIOTECS alliance between the Technische Universität Braunschweig and the Leibniz Universität Hannover. This initiative is supported by the Ministry of Science and Culture (MWK) of Lower Saxony, Germany. This project has also received funding from the European Research Council (ERC) under the European Union's Horizon 2020 research and innovation programme (grant agreement No 757490).

Competing interests

The authors declare no competing interests.

Abbreviations

TS, tropolone sesquiterpenoids; EPO, erythropoiestin; CTV, cell trace violet; MFI, mean fluorescence intensity

FIG. LEGENDS

Figure 6: Alterations of cell morphology of FAIK3-5 cells after 24 h of treatment with the TS compounds pycnidione (**1**), eupenifeldin (**2**)**,** xenovulene B (**3**), 4-hydroxyxenovulene B (**4**) and 4-dehydroxy norpycnidione (**5**). **(a)** Brightfield images (1 x 10x and 2 x 20x resolution from top to bottom) of samples treated for 24h with compound **1**-**5**. Red arrows indicate enlarged, flat and highly granulated cells that were visible to varying degrees in each treated sample. **(b)** Visualization of TS-treated cells in PhenoPlot, in which quantifiable cell features such as cell width and length, relative area of protrusions as well as their proportion and size (spike fraction and spike height) are displayed for each sample condition. In order to emphasize main differences between different treatments relative protrusion areas, spike fractions and spike height are coloured in dark green (pycnidione (**1**)), yellow (eupenifeldin (**2**)), light blue (xenovulene B (**3**)), dark blue (4-hydroxyxenovulene B (**4**)) and light green (4-dehydroxy norpycnidione (**5**)). **(c)** Multiple comparison analysis for analysed shape descriptors and morphometric parameters (cell area, aspect ratio, perimeter, relative protrusion area as well as length and number of protrusions/branches and branch junctions) were measured on at least 20 cells of pictures from three independent experiments in Fiji (version 1.53c). Statistical analysis of data was conducted with R (version 4.2.1). All parameters marked with (†) are not depicted in PhenoPlot graphs. Significances range from $p > 0.05$ (NS), 0.05 - 0.01 (*), < 0.01 - 0.001 (**) to < 0.001 (***). The estimated contrasts and corresponding confidence intervals are given in Supplementary Information S9 and S10.

Figure 7: Proliferation deceleration of FAIK3-5 cells after treatment with pycnidione (**1**), eupenifeldin (**2**), xenovulene B (**3**), 4-hydroxyxenovulene B (**4**) and 4-dehydroxy norpycnidione (**5**) compared to untreated controls and tropolone moiety lacking compound 4-hydroxy

norxenovulene B (**6**). Statistics were calculated based on normalized values of obtained ln-transformed mean fluorescence intensities (MFIs) directly after cell trace violet (CTV) staining of the undivided population and 24h post compound treatment. **(a)** Graphical overview show normalized MFI values of three biological replicates (● = 1,▲ = 2, ■ = 3) after treatment with compounds **1** - **6** and the untreated control sample, as well as their modelled means (black dots) and pointwise 95% confidence intervals. Treatments marked with the same letter do not differ significantly from each other ($\alpha = 0.05$). **(b)** Histograms and obtained fluorescence intensities of CTV stained FAIK3-5 cells show MFI peaks and values of starting intensities of undivided cell populations at d1 (grey background), control peaks of untreated samples at d3 (red) and MFI peaks of the respective compounds used for treatment (dark green = pycnidione (**1**), yellow = eupenifeldin (**2**), light blue = xenovulene B (**3**), dark blue = 4-hydroxyxenovulene B (**4**), light green = 4-dehydroxy norpycnidione (**5**), 4 grey = 4-hydroxy norxenovulene B (**6**)). **(c)** Pairwise mean comparisons showed significant differences in normalized MFI values between all TS compounds treated cells compared to untreated controls and compound 4-hydroxy norxenovulene B (**6**). Black dots indicate back transformed means of calculated ratios and their 95% confidence intervals (blue bars). Respective p-values for each calculation are displayed on the right side. The estimated contrasts and corresponding confidence intervals are given in Supplementary Information S11 and S12.

Figure 8: Cell viability of FAIK3-5 cells after treatment with pycnidione (**1**), eupenifeldin (**2**), xenovulene B (**3**), 4-hydroxyxenovulene B (**4**) and 4-dehydroxy norpycnidione (**5**) for 24 h and compared to untreated controls and tropolone moiety lacking compound 4-hydroxy norxenovulene B (**6**). Statistical analysis was conducted based on the calculation of the average proportion of dead

cells per samples (samples size = 10.000 cells). **(a)** Proportions of dead cells (black dots) and their pointwise 95 % confidence intervals (error bars) of three biological replicates (● = 1, ▲ = 2, ■ = 3). Treatments marked with the same letter do not differ significantly from each other (α = 0.05). **(b)** Multiple comparisons of calculated odds ratios (black dots) and simultaneous 95 % confidence intervals (blue bars, details see Supplementary Information S14) showing differences of cell survival between samples treated with tropolone moiety containing compounds (**1** – **5**) compared to untreated samples or tropolone-lacking compound **6**. P-values for each contrast test of different treatments are displayed on the right side. **(c)** Representative plot of fluorescent intensities of SYTOX™ AADvanced™ stained FAIK3-5 cells samples. Each plot displays percentages of living and dead populations in an untreated control sample and after treatment with and the TS compounds pycnidione (**1**), eupenifeldin (**2**), xenovulene B (**3**) and 4-hydroxyxenovulene B (**4**) and 4-dehydroxy norpycnidione (**5**)**,** and tropolone lacking compound 4-hydroxy norxenovulene B (**6**). Peaks of fluorescence intensities are displayed with the respective living / dead control (red) containing a heat-killed dead cell population.

Figure 9: Erythropoietin (EPO) content of FAIK3-5 samples treated with the tropolone sesquiterpenoids (TS) pycnidione (**1**), eupenifeldin (**2**), xenovulene B (**3**), 4-hydroxyxenovulene B (**4**), 4-dehydroxy norpycnidione (**5**) and tropolone-lacking compound 4-hydroxy norxenovulene B (**6**) and their respective vehicle controls (DMSO 0.6% (*v/v*), DMSO 1.2 % (*v/v*)). **(a)** EPO protein concentrations measured in three biological replicates (● = 1,▲ = 2, ■ = 3) of FAIK3-5 cells treated with 6 µM of TS compounds **1**, **2**, **3**, tropolone- moiety lacking compound **6** and their respective DMSO vehicle control (0.6 % (*v/v*)) or 12 µM of TS compounds **4**, **5**, and their respective DMSO vehicle control (1.2 % (v/v)) without pre-treatment of 5-Azacytidine (5-Aza). Block dots are indicating the model based least square means and their pointwise 95% confidence

intervals (black bars). **(b)** Measurement of basic EPO protein content in FAIK3-5 DMSO vehicle controls (0.6 % (*v/v*) and 1.2 % (*v/v*) with and without 5-Aza treatment for 6 days. Error bars indicate the standard deviation of mean EPO concentrations. **(c)** EPO protein concentrations measured in three biological replicates (● = 1,▲ = 2, ■ = 3) of FAIK3-5 cells treated with 6 µM of TS compounds **1**, **2**, **3**, tropolone- moiety lacking compound **6** and their respective DMSO vehicle control (0.6 % (*v/v*)), or 12 µM of TS compounds **4**, **5**, and their respective DMSO vehicle control (1.2 % (v/v)) with pre-treatment of 5-Azacytidine (+ 5-Aza). Block dots are indicating the model based least square means and their pointwise 95% confidence intervals (black bars). Treatments marked with ***** are significantly different from their respective vehicle controls. **(d)** Pairwise mean comparisons showed significant differences in EPO protein concentrations 4-hydroxyxenovulene B (**4**), 4-dehydroxy norpycnidione (**5**) and eupenifeldin (**2**) compared to their respective vehicle controls. Black dots indicate back transformed means of measured EPO concentrations and their 95% confidence intervals (blue bars). Respective p-values for each calculation are displayed on the right side. The estimated contrasts and corresponding confidence intervals are given in the Supplementary Information S16.

Figure 10: Stereochemistry of selected tropolone sesquiterpene (TS) compounds (**1**-**5**) and control compound (**6**) lacking a tropolone moiety [32]. Key features are highlighted in red (= polyketide derived tropolones), blue (= benzopyranyl moiety) and grey (C-10 hydroxylation).